

Effect of the Chain-Length Compatibility of Surfactants and Mechanical Properties of Mixed Micelles on Surfaces

Yakov I. Rabinovich,^{*,†} Samir Pandey,[‡] Dinesh O. Shah,^{‡,§,||} and Brij M. Moudgil^{*,†,⊥}

Particle Engineering Research Center, Center for Surface Science & Engineering, Department of Chemical Engineering, Department of Anesthesiology, and Departments of Materials Science and Engineering, University of Florida, Gainesville, Florida 32611-6135

Received October 25, 2005. In Final Form: March 16, 2006

Force/distance curves for silicon nitride tip/flat silica or alumina coated by a layer of mixed micelles of cationic/anionic surfactant are measured by using AFM. Mixtures of SDS/ C_n TAB (with molecular ratios of 3:1 and 20:1) and C_n TAB/SDS (with molecular ratio of 85:15) were used for alumina and silica substrates, respectively. The number of carbon atoms per C_n TAB molecule, n , was in the range of 8 to 16. On the basis of the force/distance curves, the elastic modulus, E , and yield strength, Y , of surface micelles are calculated. It is shown that in surfactant mixtures containing SDS the maximal repulsive force (the barrier F^{bar}) at which the tip punctured the micelles, as well as the magnitudes of E and Y , attained the maximal values for C_{12} TAB (i.e., when the hydrocarbon chain lengths of two oppositely charged surfactants are the same). Obviously, it can be related to the highest density structure of these micelles. Note that the literature data for the surface micelles from pure C_n TAB solutions demonstrate a monotonic dependence of F^{bar} , E , and Y on n in the range of $n = 8-16$, whereas the oppositely charged mixed surfactant systems yield much higher values of F^{bar} , E , and Y than does an equivalent chain length from the homologue series plots. The results obtained for mechanical characteristics of mixed micelles at the surface are compared with the results for the relaxation time, τ_2 , that characterizes the lifetime (and therefore structure) of the bulk micelles. Both the dependence of F^{bar} , E , and Y on n for the surface mixed micelles and τ_2 on n for the bulk mixed micelles demonstrate a maximum at $n = 12$ for the C_n TAB + SDS system. This correlation between properties of the surface and bulk micelles suggests that the mechanical properties of the surface micelles are largely determined by the interactions between surfactant molecules with surfactant–substrate interactions playing a secondary role.

Introduction

Steric forces between solids separated by one or two layers of the micelles adsorbed or settled on solids from solutions near and above the critical micelle concentration (cmc) have been measured using atomic force microscopy (AFM). For example, the force/distance dependencies and mechanical/thermodynamic characteristics of the surfactant monomers or micelles coating the solid surfaces were investigated by various authors.^{1–7} The concentration regime in which surfactants become the effective dispersant and the process of self-assembly have been described in detail elsewhere.^{8,9} The direct images of surface micelles on the solid/liquid interface obtained with AFM have been reported in the literature,^{10,11} and the different structures of the surface

micelles were investigated by many authors.^{12–17} The properties of micellar layers were measured for pure cationic and anionic surfactants and for their mixtures as well.¹ It was shown that adding C_{12} TAB to SDS solutions gives rise to a sharp decrease in the SDS concentration at which the strong steric force appears. Moreover, the barrier (i.e., the maximal repulsive force) increased significantly for the surfactant mixture as compared with the single surfactants. It was explained by a denser packing of micelles owing to reduced repulsive forces between the charged head-groups of mixed micelles upon introduction of the oppositely charged groups.

Note that force/distance curves allow the calculation of mechanical and thermodynamic properties, as suggested in ref 6. It was shown that the barrier height F^{bar} can be used for the yield strength calculation, Y , and the slope of the steric portion of the curve can be employed for the elastic modulus, E . In the present article, the effect of the hydrocarbon chain length compatibility of two oppositely charged surfactant monomers in their mixture is investigated. This problem is also considered in ref 18 for C_n TAB/SDS mixtures for the properties of the bulk micelles (as relaxation time τ_1 and τ_2) and mixed monomers at the air/solution interface (as surface tension and surface viscosity). In ref 18, the pressure-jump method was used for investigations of τ_2 of the bulk micelles. It was shown that maximal values of these parameters of the bulk micelles occur near $n = 12$ (i.e.,

* Corresponding author. E-mail: bmoudgil@erc.ufl.edu. Tel: (352) 846-1194. Fax: (352) 846-1196.

[†] Particle Engineering Research Center.

[‡] Center for Surface Science & Engineering.

[§] Department of Chemical Engineering.

^{||} Department of Anesthesiology.

[⊥] Departments of Materials Science and Engineering.

(1) Adler, J. J.; Singh, P. K.; Patist, A.; Rabinovich, Y. I.; Shah, D. O.; Moudgil, B. M. *Langmuir* **2000**, *16*, 7255.

(2) Singh, P. K.; Adler, J. J.; Rabinovich, Y. I.; Moudgil, B. M. *Langmuir* **2001**, *17*, 468.

(3) Pashley, R. M.; McGuiggan, P. M.; Horn, R. G.; Ninham, B. W. *J. Colloid Interface Sci.* **1988**, *125*, 569.

(4) Kekicheff, P.; Christenson, H. K.; Ninham, B. W. *Colloids Surf., A* **1989**, *40*, 31.

(5) Rutland, M. W.; Parker, J. L. *Langmuir* **1994**, *10*, 1110.

(6) Rabinovich, Y. I.; Vakarelski, I. U.; Brown, S. C.; Singh, P. K.; Moudgil, B. M. *J. Colloid Interface Sci.* **2004**, *270*, 29.

(7) Subramanian, V.; Ducker, W. J. *Phys. Chem. B* **2001**, *105*, 1389.

(8) Fuerstenau, D. W.; Healy, T. W.; Somasundaran, P. *Trans. AIME* **1964**, *229*, 321.

(9) Scamehorn, J. F.; Schecter, R. S.; Wade, W. H. *J. Colloid Interface Sci.* **1981**, *85*, 463. Scamehorn, J. F.; Schecter, R. S.; Wade, W. H. *J. Colloid Interface Sci.* **1981**, *85*, 479. Scamehorn, J. F.; Schecter, R. S.; Wade, W. H. *J. Colloid Interface Sci.* **1981**, *85*, 494.

(10) Manne, S.; Cleveland, J. P.; Gaub, H. E.; Stucky, G. S.; Hansma, P. K. *Langmuir* **1994**, *10*, 4409.

(11) Manne, S.; Gaub, H. E. *Science* **1995**, *270*, 1480.

(12) Aksay, I. A.; Trau, M.; Manne, S.; Honma, I.; Yao, N.; Zhou, L.; Fenter, P.; Eisenberger, P. M.; Gruner, S. M. *Science* **1996**, *273*, 892.

(13) Wanless, E. J.; Davey, T. W.; Ducker, W. A. *Langmuir* **1997**, *13*, 4223.

(14) Ducker, W. A.; Wanless, E. J. *Langmuir* **1999**, *15*, 160.

(15) Patrick, H. N.; Warr, G. G.; Manne, S.; Aksay, I. A. *Langmuir* **1999**, *15*, 1685.

(16) Fielden, M. L.; Claesson, P.; Verrall, R. E. *Langmuir* **1999**, *15*, 3924.

(17) Velegol, S. B.; Fleming, B. D.; Biggs, S.; Wanless, E. J.; Tilton, R. D. *Langmuir* **2000**, *16*, 2548.

Table 1. Composition of the Micellar Solutions and Flat Substrates Used for the Investigation of the Mechanical Properties of Micelles^a

<i>N</i>	composition	substrate
1	1 mM SDS + 0.33 mM C _{<i>n</i>} TAB + 0.1 M NaCl	alumina
2	16.7 mM SDS + 0.83 mM C _{<i>n</i>} TAB	alumina
3	2 cmc C _{<i>n</i>} TAB + 15 mol % SDS	silica

^a All solutions are at pH 5.8.

when the length of hydrocarbon chain of C_{*n*}TAB coincided with the chain length of the SDS molecule).

It is not known at this point whether there is any correlation between the properties of adsorbed micelles and the properties of micelles in solution. Thus, the present article is dedicated to the AFM force measurements for the SDS + C_{*n*}TAB (for *n* = 8–16) mixed surfactant system near and above the cmc. The comparison of the properties of the mixed micelles at the surface obtained in the present article and the properties of the mixed micelles in bulk solution obtained from the literature may allow one to gain additional insight regarding the breakage of the micelles on surfaces when two solid surfaces approach each other. These data may be useful for various technological processes such as grinding, polishing, dispersion, and boundary lubrication.

Materials and Methods

The use of AFM for force/distance measurements is well known.¹⁹ Interaction force measurements were carried out with smooth, flat substrates of silica or alumina in a fused-silica liquid cell with a Digital Instruments (DI) Nanoscope III atomic force microscope. The probes used in this study were DI triangular oxide sharpened contact-mode cantilevers (NP-S type, 200 μm long and thick-legged; stiffness *k* = 0.12 N/m, radius of the silicon nitride tip ca. 15 nm). The silica wafers were provided by Dr. Arwin (Linköping University, Sweden), and the basal plane (*C* plane) alumina substrates were obtained from MTI Corporation (Richmond, CA).

The procedures for the force measurements and the generation of the force/distance curves in the presence of self-assembled surfactant aggregates have been reported previously.^{1,2} The silica and alumina substrates were cleaned with reagent-grade acetone followed by methanol and subsequent boiling in Millipore water for several hours prior to use. All measurements in surfactant solutions were carried out after 10–15 min of adsorption time. To remove the surfactant after the experimental series with each solution, the chamber (with samples) was cleaned with Millipore water and checked for the lack of remaining surfactant by measuring the force/distance curve.

The radii of all AFM tips used in the experiments were determined through scanning electron microscope (SEM) images.

Trimethylammonium bromide surfactants of varying chain length (C_{8–16}TAB) and 99% purity were obtained from TCI America. The sodium dodecyl sulfate (SDS) was 99% pure as received from Aldrich Chemical Co. The dependencies of surface tension versus the log of the concentration for the surfactants did not show a depression in the vicinity of the cmc, indicating that the reagents used were of high purity. The cmc's were also in good agreement with reported literature values.²⁰ All other reagents used were of at least 98% purity and were obtained from Fisher Scientific Co. The water used in the experiments was produced by a Millipore filtration system and had an internal specific resistance of 18.2 MΩ and less than 7 ppb carbon.

The compositions of three solutions in which the tip/micelles interactions were studied are given in Table 1. The first solution (1

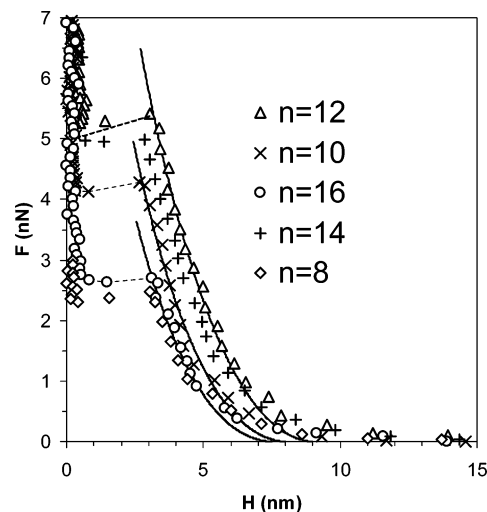


Figure 1. *F* vs *H* for alumina in a solution of 1 mM SDS + 0.33 mM C_{*n*}TAB + 0.1 M NaCl, pH 5.8. Theoretical fitting curves (solid lines, Hertz theory) are plotted with eqs 1–6 for *n* = 10, 12, and 16.

mM SDS + 0.33 nM C_{*n*}TAB + 0.1 mM NaCl) was chosen because the highest density micelles structure is achieved at a 3:1 molecular ratio of the concentrations of two oppositely charged surfactants. The second solution (16.7 mM SDS + 0.83 mM C_{*n*}TAB, no electrolyte) presents a composition with a small content of CTAB (1 to 20), and the third solution ((2cmc C_{*n*}TAB + 15 mol % SDS) has a composition close to the most dense micelle structure (with a 5:1 molecular ratio of two surfactants). The first two solutions were used for the alumina substrate because their main component was SDS, and the third solution was used for the silica substrate because its main component was C_{*n*}TAB, which adsorbed onto silica.

Results and Discussion

Figure 1 represents typical force/distance curves for the interaction of the AFM tip with a flat substrate under a surfactant solution. At large separation distances, the ion-electrostatic force between micelles and the tip plays a certain role whereas for shorter distances the steric force becomes dominant. For example, for the surfactant solution with *n* = 12 in Figure 1, only the steric force acts below an approximately 6 nm distance. The role of DLVO forces will be discussed below. When the loading force reaches a certain critical magnitude (which we call the “barrier”, *F*^{bar}), the tip penetrates and breaks the adsorbed micellar layer. The values of the barrier force, *F*^{bar}, elastic modulus, *E*, and yield strength, *Y*, can be used as characteristics of the surface micelles. The calculations of *E* and *Y* will be explained below.

Figures 1–3 represent force/distance curves obtained for different substrate materials and mixed surfactant solutions. Figures 1 and 2 are plotted for an alumina surface under solutions with compositions of 1 mM SDS + 0.33 mM C_{*n*}TAB + 0.1 M NaCl and 16.7 mM SDS + 0.83 mM C_{*n*}TAB (without electrolyte), respectively. Results for these solutions were obtained for values of *n* ranging from 8 to 16; however, only a few experimental curves are shown in these Figures for clarity. Figure 3 is obtained for a silica substrate under a solution of 2 cmc C_{*n*}TAB + 15 mol % SDS. For comparison, the curves are also given for the solutions of 2 cmc C₁₂TAB or C₁₀TAB (without SDS). No electrolyte was used for the solutions shown in Figure 3. It appears from Figure 3 that *F*^{bar} for the mixed surfactants is significantly higher than for pure surfactants. In Figure 3, the results without SDS are shown only for C₁₂TAB and C₁₀TAB. For 2 cmc C₈TAB without SDS, we could not see the rupture of micelles, probably because of the lack of sensitivity of the cantilever. For SDS without C_{*n*}TAB, the value of *F*^{bar} for silica is smaller because of the small

(18) Patist, A.; Chhabra, V.; Pagidipati, R.; Shah, R.; Shah, D. O. *Langmuir* **1997**, *13*, 432.

(19) Ducker, W. A.; Senden, T. J. *Langmuir* **1992**, *8*, 1831.

(20) Rosen, M. J. *Surfactants and Interfacial Phenomena*, 2nd ed.; Wiley: New York, 1989.

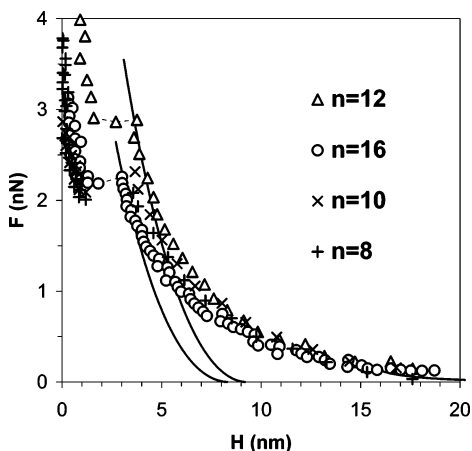


Figure 2. F vs H for alumina in a solution of 16.7 mM SDS + 0.83 mM C_n TAB. No electrolyte, pH 5.8. Theoretical fitting curves (solid lines, Hertz theory) are given only for $n = 12$ and 16. The solid line in the lower right corner represents the DLVO force for $\psi = 60$ mV, $C = 0.01$ M, and $l_1 = 15$ nm.

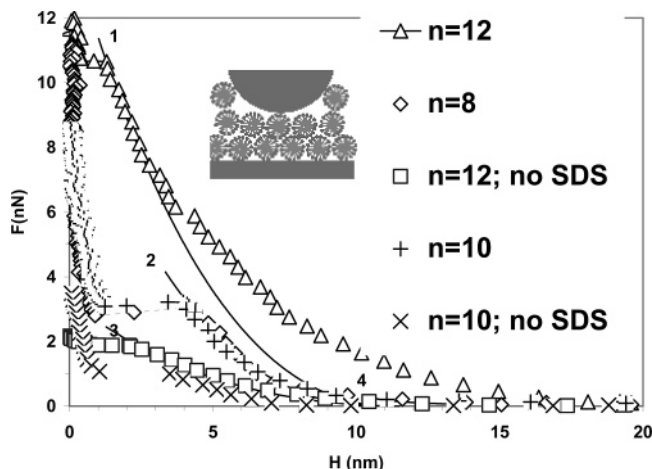


Figure 3. F vs H for silica in a solution of 2 cmc C_n TAB + 15 mol % SDS and 2 cmc C_{12} TAB and C_{10} TAB (without SDS). Theoretical curves 1 and 2 (Hertz theory) are plotted for C_{12} TAB + 15 mol % SDS and C_8 TAB + 15 mol % SDS, respectively. Hertz curve 3 is plotted for C_{12} TAB without SDS. Theoretical curve 4 is plotted for DLVO forces with $l_1 = 10$ nm, $\psi = 90$ mV, and $C = 0.01$ M. No electrolyte, pH 5.8. The inset is the model of two micelle layers between the flat substrate and the tip.

adsorption of SDS on silica. Note also that for the solution of 2 cmc C_n TAB/15 mol % SDS the results could be obtained only for $n = 8-14$. We could not get reproducible results for $n = 16$, a possible reason for which could be the fast precipitation from the solution over time. All solutions in Figures 1–3 were at pH 5.8. The points in these Figures are experimental results, whereas solid lines are theoretical graphs that will be explained below.

Apart from providing information about the barrier values, the experimental force/distance graphs (Figures 1–3) also allow the calculation of the elastic (Hertz) modulus, E , and yield strength, Y , as described in ref 6.

It is noted that the end of the tip has a semispherical shape and the radius of the extra-sharp tip is about $R = 15$ nm. Another interacting surface, the surface of the micelle layer, consists of spheres of radius near 3 to 4 nm. The model of the steric interaction of the spherical tip with many spherical micelles of the smaller radius would be rather complex. Therefore, we used the sphere/flat model for the Hertz interaction, where we assume the surface of the micelle layer to be flat. This approximation may account

for the possible deviation of the theoretical results from the experimental force/distance curves.

Calculation of E and Y

As the AFM tip with radius R is pressed against the flat surfactant layer with a force F , it contacts an area of radius a and has a penetration depth of δ . From the classical Hertz theory,²¹ the relationship between F and a for the case of a rigid sphere and an infinite half space of elastic (Young's) modulus E and Poisson ratio ν is found to be

$$F^H = \frac{3Ea^3}{2(1-\nu^2)R} \quad (1)$$

For δ^H and a , the following equation is valid:

$$\delta^H = \frac{a^2}{R} \quad (2)$$

The superscript H is used to denote the use of Hertz theory. From eqs 1 and 2, F^H can be derived to be

$$F^H = \left[\frac{3E}{2(1-\nu^2)} \right] R^{0.5} \delta^{H 1.5} \quad (3)$$

The yield stress of the layer, Y , can be obtained as

$$Y = \frac{3F_m}{2\pi a_m^2} \quad (4)$$

where F_m and a_m are the force and the contact radius at the point of rupture of the layer.

For the layer with finite thickness h_0 , the Hertz theory is valid only if $a/h_0 \ll 1$. To account for the role of the small thickness or the large contact radius, Shull et al.^{22,23} proposed a semiempirical correction term to the Hertz equation as follows

$$\delta = \delta^H \left(0.4 + 0.6 \exp\left(-\frac{1.8a}{h_0}\right) \right) \quad (5)$$

and

$$F = F^H \left(1 + 0.15 \left(\frac{a}{h_0} \right)^3 \right) \quad (6)$$

where F^H and δ^H are as defined by eqs 1 and 2. At small values of a/h_0 , eqs 5 and 6 converge to the Hertz theory.

In Figures 1–3, the solid curves are plotted using eqs 1–6 (i.e., for Shull's approach). The values of E and h_0 are used as fitting parameters. Choosing the values of E and h_0 , the value of a was calculated as a function of F using Shull's equations (eqs 5 and 6), as described in ref 6. Note that the fit of the experimental curves is better for Figure 1 and significantly worse for Figures 2 and 3. In the last two cases, only the upper parts of the curves (before the jump) can be fitted by eqs 1–6. To explain the "tails" of graphs F versus H in Figures 2 and 3, we calculated the DLVO force as

$$F_{DLVO}(H) = F_{el}(H - l_1) + F_{dis}(H) \quad (7)$$

where F_{el} and F_{dis} are the ion-electrostatic (electrical double layer) force and the dispersion force, respectively. Note that

(21) Hertz, H. *Miscellaneous Papers*; McMillan: London, 1986.
 (22) Shull, K. R.; Ahn, D.; Mowery, C. L. *Langmuir* **1997**, *13*, 1799.
 (23) Shull, K. R.; Dongchan, A.; Chen, W. C.; Flanigan, C. M.; Crosby, A. J. *Macromol. Chem. Phys.* **1998**, *199*, 489.

distance l_1 includes the thickness of the micellar layer on the flat substrate, l_0 , and possibly the thickness of the micellar layer on the semispherical tip. The ion-electrostatic force was calculated for the constant-charge condition using the algorithm suggested by D. Chan et al.²⁴ and the dispersion force was calculated with the following simplest London–Hamaker equation and Derjaguin's approximation^{25,26}

$$F_{\text{disp}}(H) = \frac{AR}{6H^2} \quad (8)$$

The values of the electrostatic potential ψ ($H = \infty$), the electrolyte concentration C , and the distance l_1 are given in the Figure captions. The value of ψ was optimized for the best agreement between theory and experiment at large distances between the two approaching surfaces. The Hamaker constant value for the interaction of the substrate/micelles/water/micelles/tip was less than $A = 1 \times 10^{-20}$ J. As it appears from Figures 2 and 3, the experimental dependence of F versus H for low electrolyte concentrations at large distances between samples can actually be explained by DLVO forces (curve in the bottom right corner in Figure 2 and curve 4 in Figure 3). Moreover, a slight shift in the shape of the curves for $C_{12}\text{TAB} + \text{SDS}$ in Figure 3 and possibly for $\text{SDS} + C_n\text{TAB}$ in Figure 2 indicates the existence of the second layer of micelles between the samples. From these Figures, it also follows that the whole range of distances can be approximately separated into two zones where DLVO or steric forces dominate, respectively. The calculation of interacting forces, including ion-electrostatic and elastic forces, is given in detail in ref 27. Calculations of forces between a hard-sphere sample and a deformable water surface are given in ref 28.

The good agreement of the Hertz theory with experimental results in Figure 1 and worse agreement with Figures 2 and 3 are related to the fact that Figure 1 is obtained for solutions with additional 0.1 M NaCl whereas Figures 2 and 3 are obtained for a solution without additional electrolyte. As a result, the Debye radii in Figures 2 and 3 are very large, and the ion-electrostatic force between the tip and the micellar layer acts up to relatively longer distances. However, at shorter distances ($H = 3$ to 4 nm in Figure 2 and 1 to 4 nm in Figure 3 for $C_{12}\text{TAB} + \text{SDS}$), where the steric force becomes dominant, the quality of the fit with eqs 1–6 is improved significantly.

As mentioned above, the long-range forces from curve 1 in Figure 3 can be explained (besides the ion-electrostatic force) by the existence of the second micellar layer. Actually, the surface of the Si_3N_4 tip at pH 5.8 is negative. As a result, the micelles consisting mainly of $C_n\text{TAB}$ can adsorb onto the tip. However, we found that SDS also adsorbs onto Si_3N_4 . This may give rise to the existence of two layers of micelles between the samples (on the flat substrate and on the tip). In our opinion, the layer on the tip should be much weaker than the layer on the flat surface because the layer on the tip is expected to migrate away under pressure. However, the long-distance part of the force/distance curve may be attributed not only to the DLVO forces (curve 4) but also to the presence of the second layer of micelles.

Using Figures 1–3, we obtained values of F^{bar} at distances near 2 to 3 nm. At shorter distances, the AFM tip jumped into contact with the flat substrate (shown by the dashed lines in

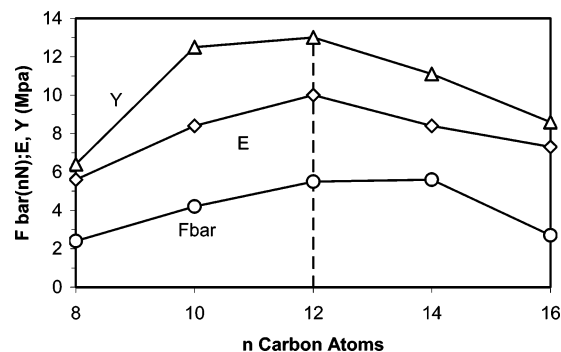


Figure 4. Force at the rupture, F^{bar} , elastic modulus, E , and yield strength, Y , of micelles for alumina in a solution of 1 mM SDS + 0.33 mM $C_n\text{TAB}$ + 0.1 M NaCl. Results are calculated with eqs 1–6 (Shull's approach). The vertical dashed line shows $n = 12$ where the length of the $C_{12}\text{TAB}$ molecule is equal to the length of the SDS molecule.

Figures 1–3), which reflects the breakage of the micellar layer. At these short distances, because of the lack of a micellar layer, the Hertz–Shull theory is not valid anymore, and the experimental points deviate from the theoretical curves (solid lines) in the Figures.

The distance between the substrate (alumina or silica) and the tip at the position of their contact (rather than the jump-in distance) should be equal to the micelles' size (plus possibly the solvation layer). In principle, this means that the distance l_0 should be equal to the micellar size. As follows from Figure 1, this is more or less correct for solutions with high electrolyte concentrations. However, for the smaller electrolyte concentrations (Figures 2 and 3), the maximum distance at which the forces still act are significantly larger than the micellar size and l_0 . This can be due to the existence of the second layer of the micelles on the tip and to the ion-electrostatic force (Figures 2 and 3), which acts before direct contact between the tip and the micelle layer. The inset in Figure 3 shows the suggested model of two micellar layers between the tip and the flat substrate. The discussion of the existence and properties of the second layer of micelles (on the tip) is beyond the scope of this article. Here we note only that the presence of this layer is more probable under the lower-concentration electrolyte solution because at higher concentrations the counterions adsorb onto the surface and decrease the probability of micelle adsorption.

Regarding the jump-in distance, this is the distance at which the loading force (possibly including the van der Waals and hydrophobic forces if any) measured by the AFM reaches the value determined by the yield stress. Therefore, the jump-in distance depends not only on the micellar size but also on the micelle elasticity and strength.

Fitting the experimental curves with eqs 1–6, we also calculated the values of E and Y . Each value of F^{bar} reported is the average value from several experiments, and values of E and Y were calculated from the F versus H graphs. The results for F^{bar} , E , and Y values obtained from force–distance curves are given in Figures 4–6 as a function of the hydrocarbon chain length, n , of $C_n\text{TAB}$ in mixtures with SDS. It is to be noted that the actual values of F^{bar} , E , and Y shown in Figures 4–6 may not be compared precisely across the Figures because of possible differences in the tip and cantilever used in each set of experiments. However, the variation of the properties within a Figure is reliable because the same tip and the same cantilever are used for the whole set of experiments.

From Figures 4–6, it appears that for all mixed surfactant solutions the values of the F^{bar} , E , and Y reach their maximal magnitudes at $n = 12$. This means that the mixed micelles at the surface have the maximal strength when the length of the

(24) Chan, D. Y. C.; Pashley, R. M.; White, L. R. *J. Colloid Interface Sci.* **1980**, *77*, 283.

(25) Hamaker, H. C. *Physica* **1937**, *4*, 1058.

(26) Derjaguin, B. V. *Kolloidzeitschrift* **1934**, *69*, 155.

(27) Vakarelski, I. U.; Toritani, A.; Nakayama, M.; Higashitani, K. *Langmuir* **2003**, *19*, 110.

(28) Chan, D. Y. C.; Dagastine, R. R.; White, L. R. *J. Colloid Interface Sci.* **2001**, *236*, 141.

(29) Vakarelski, I. U.; Brown, S. C.; Rabinovich, Y. I.; Moudgil, B. M. *Langmuir* **2004**, *20*, 1724.

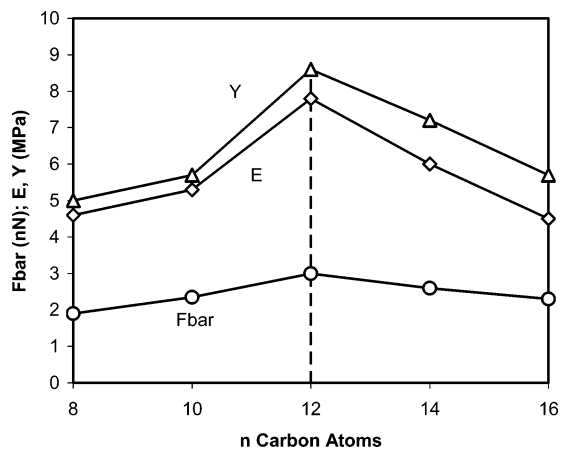


Figure 5. Force at the rupture, F^{bar} , elastic modulus, E , and yield strength, Y , of micelles for alumina in a solution of 16.7 mM SDS + 0.83 mM C_n TAB (no electrolyte). The vertical dashed line shows $n = 12$ where the length of the C_{12} TAB molecule is equal to the length of the SDS molecule.

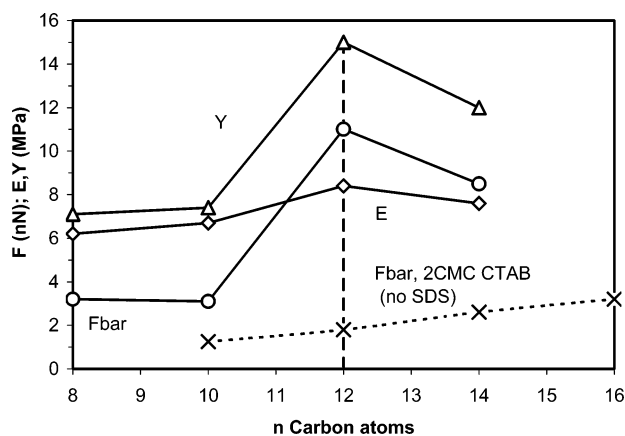


Figure 6. Force at the rupture, F^{bar} , elastic modulus, E , and yield strength, Y , of the micelles for silica in a solution of 2 cmc C_n TAB + 15 mol % SDS. For comparison, the values of F^{bar} for pure 2 cmc C_n TAB (dashed line, data are taken from ref 1) are given. The vertical dashed line shows $n = 12$ where the length of the C_{12} TAB molecule is equal to the length of the SDS molecule.

hydrocarbon chains of the cationic surfactant is the same as the chain length of the anionic surfactant. It is related to the tightly packed molecular structure of the mixed micelles. The comparison of results for F^{bar} for C_n TAB/SDS mixtures and for pure 2 cmc C_n TAB (dashed line in Figure 6, these results are taken from ref 1) shows that the magnitudes of F^{bar} for the mixed surfactant systems are several times higher than for pure C_n TAB. Moreover, as distinct from the mixed micelles, the dependence of F^{bar} on n for pure C_n TAB is monotonic. Both findings are in close agreement with the results from ref 18, which show a similar optimum behavior for a number of bulk and air/water interface properties when the chain length of the main surfactant SDS was equal to the chain length of the cosurfactant C_n TAB. This behavior of the bulk micelles was attributed in ref 18 to the molecular structure at $n = 12$ due to the tight packing of the chains of surfactant and cosurfactant of equal length. For unequal chains, the additional portion of the chains perturbs the molecular packing by its thermal motion.

This conclusion about the properties of the bulk and the surface mixed micelles near $n = 12$ (when the lengths of the hydrocarbon chains of surfactants and cosurfactants are equal) is important for understanding the effect of the chain length compatibility of surfactants in a mixture. Moreover, it is also important for the investigation of the reason that surface micelles break under

loading. Results presented in Figures 1–3 and many other results in the literature indicate that after the loading force reaches a certain critical value (barrier) the tip jumps into contact with the flat solid substrate. There can be three possible reasons for this jump: desorption, breakage of micelles under tip pressure, and the side shift of micelles. We believe that the third reason can play a role only at relatively lower concentrations of micelles. For the full surface layer of micelles, the barrier reaches the saturation (maximal) value because there is no available space between micelles to move.¹ The penetration of the tip between spherical micelles (i.e., the side shift of micelles under tip pressure) does not seem to occur. Actually, in the case of this type of shift, the mechanical properties of the micelle layer would depend on the adsorption energy (which monotonically increases with chain length) rather than on the structure of the micelles themselves (which is demonstrated by a maximum for equal chain lengths of mixed surfactants). The reason for the absence of the shift is related to the dense layer of the micelles at 2 cmc and to the large radius of the probe (tip) as compared to that of the micelles. For lower concentrations of surfactants or a weak energy of adsorption, the side shift and desorption effects could be more important than the strength of the structure of micelles.

As mentioned above, in ref 18 the authors investigated the properties of the bulk micelles of mixed surfactants systems. In particular, it was shown that the values of the relaxation time τ_2 (which characterize the time of the spontaneous breakage of the bulk micelle) have a maximum near $n = 12$ (for mixtures of C_n TAB and SDS). A comparison of the results in Figures 4–6 with this result for τ_2 demonstrates a qualitative correlation between our result (for the surface micelles) and the results of ref 18 (for the bulk micelles). It is clear that the adsorption energy of the surface micelles and the distance between the adsorption sites on the solid substrate cannot play any role in the case of the bulk micelles. Therefore, the similarity of the properties of the surface and the bulk micelles proves that the jump in the force/distance curves for the surface micelles may be explained by the breakage of the micelles rather than their shifting or desorption. If this is true, then in the present system the value of F^{bar} is primarily determined by the micellar structure with the adsorption energy of the surfactant playing a secondary role. Indirectly, the conclusion about the breakage (rather than desorption) of the surface micelles under the loading force can be reached from the results of ref 29. In this article, it was shown that even for high loading force (larger than F^{bar}) the friction coefficient between the tip and the flat substrate remained lower than the coefficient for a bare or uncoated substrate, which was attributed to the presence of a surfactant monolayer remaining on the surface even after the breakage of the micelles.

Conclusions

Mechanical properties of the micelles on the surface from two oppositely charged surfactants (CTAB and SDS) show maximal values for equal hydrocarbon chains of surfactants. The results correlate with the relaxation time data obtained in ref 18 for the bulk micelles. This correlation suggests that the micellar strength, rather than desorption of micelles, controls the breakage of micelles on the surface under load.

Acknowledgment. We acknowledge the financial support of Particle Engineering Research Center (PERC) at the University of Florida, the National Science Foundation (NSF) (grant EEC-94-02989), and the Industrial Partners of the ERC for supporting this research. Any opinions, findings, and conclusions or recommendations expressed in this material are those of the authors and do not necessarily reflect those of the National Science Foundation.